Journal of Alloys and Compounds 495 (2010) 338–340

Contents lists available at ScienceDirect

Journal of Alloys and Compounds

journal homepage: www.elsevier.com/locate/jallcom

Structural changes in Zr-based bulk metallic glasses deformed by high pressure torsion

Ádám Révész[a,*], Péter Henits[a], Zsolt Kovács[a,b]

[a] Department of Materials Physics, Eötvös University, P.O. Box 32, H-1518 Budapest, Hungary
[b] School of Electrical, Electronic & Mechanical Engineering, University College Dublin, Belfield, Dublin 4, Ireland

ARTICLE INFO

Article history:
Received 4 July 2008
Received in revised form 20 October 2009
Accepted 21 October 2009
Available online 29 October 2009

Keywords:
Metallic glasses
Mechanical properties
Synchrotron radiation
X-ray diffraction
Calorimetry

ABSTRACT

$Zr_{44}Ti_{11}Cu_{10}Ni_{10}Be_{25}$ and $Zr_{57}Ti_5Cu_{20}Al_{10}Ni_8$ bulk metallic glass disks have been subjected to severe plastic deformation by high pressure torsion. Structural changes occurred during torsion straining were detected by high intensity synchrotron X-ray diffraction, modulated thermal analysis and hardness measurements. The samples show no evidence of nanocrystallization, however, they posses atomic bond length change in the amorphous state. Simultaneously, a change in the heat capacity of the deformed state is detected which is preserved above the glass transition in the supercooled liquid range.

1. Introduction

Bulk metallic glasses (BMGs) have received increased attention from scientific and technological view points in the past couple of decades. BMGs usually posses high strength, large elastic strain limit and excellent wear resistance [1]. The deformation of BMGs is commonly described in terms of the free volume model, which predicts significant increase in atomic mobility and strong dependence of strain rate on slight change of the local free volume [2,3]. At temperatures well below the glass transition (T_g), the relative volume fraction of the plastically deformed material is very low due to the extreme localization of shear bands [4], therefore, the small contribution of plastic deformation is difficult to be detected by macroscopic methods. Recently, change in the excess free volume content on macro length scale has been studied during in situ thermal cycles by synchrotron X-ray diffraction (XRD) [5]. In these tests the excess free volume is obtained from the small increase (in the order of 10^{-3} to 10^{-4}) in the average atomic distance presuming an isotropic glass. In order to enhance the ductility of BMGs, several studies have focused on dispersing the applied strain among competitive shear band networks, either by introducing inhomogeneity in the microstructure [6] or by surface constrains techniques [7,8]. The high pressure torsion (HPT) technique, originally used for producing porosity-free bulk ultrafine-grained specimen [9], can serve as an ideal surface constrain technique to achieve extremely large plastic deformation, $\gamma = 10–100$.

Among multicomponent BMGs, Zr-based BMGs with remarkable glass forming ability have been utilized commercially to produce items for industrial applications [10]. In the present study, we demonstrate the effect of room temperature HPT deformation on $Zr_{44}Ti_{11}Cu_{10}Ni_{10}Be_{25}$ and $Zr_{57}Ti_5Cu_{20}Al_{10}Ni_8$ BMGs by applying synchrotron X-ray radiation, modulated calorimetry and microhardness tests.

2. Experimental

Commercial $Zr_{44}Ti_{11}Cu_{10}Ni_{10}Be_{25}$ (Vit 1b™, Liquidmetal Technologies Inc.) and $Zr_{57}Ti_5Cu_{20}Al_{10}Ni_8$ BMGs were subjected to HPT under constrained conditions [11]. During the HPT processing, disk-shaped samples of height 0.85 mm and radius 4 mm were strained by torsion under 8 GPa pressure $N = 2$ and 4 whole rotations between two stainless steel anvils. The optical image of a typical disk after torsion straining is seen in Fig. 1.

X-ray diffraction measurements were carried out at the ID-11 beamline of the European Synchrotron Radiation Facility (ESRF) using monochromatic photons of 90 ± 0.009 keV. The X-ray beam with a size of $10\,\mu m \times 10\,\mu m$ passed through the sample in transmission mode. Scattered intensity was collected using a CCD detector (Bruker). The 2D XRD patterns were integrated over 360° around the beam center after dark-current and spatial distortion correction using a Fit-2D software [12].

Minor differences in the thermal behaviour of the as-cast and deformed alloys were investigated by temperature modulated differential scanning calorimetry (TMDSC) in a power compensated PerkinElmer calorimeter under purified argon atmosphere. Temperature calibration was fulfilled by using pure In and Al. The heating rate was chosen 1 K/min modulated by a sine temperature oscillation with 1 K amplitude and 0.01 Hz frequency. The Fourier transformation of the heatflow rate response yields the reversing specific heat (C_p) and the total C_p is the sliding average over one modulation cycle. Microhardness (HV) testing was performed at room tem-

* Corresponding author. Tel.: +36 1 372 2823; fax: +36 1 372 2811.
E-mail address: reveszadam@ludens.elte.hu (Á. Révész).

0925-8388/$ – see front matter © 2009 Elsevier B.V. All rights reserved.
doi:10.1016/j.jallcom.2009.10.175

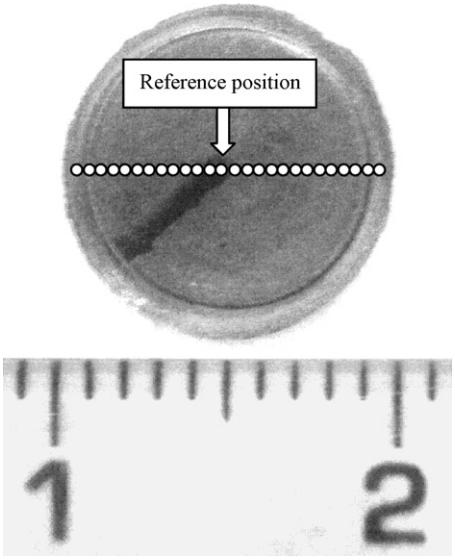

Fig. 1. A typical optical image of a $Zr_{44}Ti_{11}Cu_{10}Ni_{10}Be_{25}$ deformed by HPT during two revolutions. The circles denote the measurement positions of X-rays and HV.

perature on the polished surfaces of the disks along the diameter using a Shimadzu DUH-202 dynamic depth-sensing ultra-microhardness tester with a diamond Vickers indenter at a load rate of 17.65 mN/s up to 200 mN. During the depth-sensing hardness measurements, the indentation depth and the load were recorded as a function of time by a computer. From these data the values of HV were determined using the Oliver–Pharr method [13] by averaging 4–5 indents.

3. Results and discussion

Two-dimensional intensity distribution recorded by the CCD camera along the central line of the $Zr_{44}Ti_{11}Cu_{10}Ni_{10}Be_{25}$ and $Zr_{57}Ti_5Cu_{20}Al_{10}Ni_8$ HPT disks has shown only broad diffuse halo rings (measurement positions are marked by circles in Fig. 1), indicating that the fully amorphous structure was not destroyed during the severe plastic deformation [8,14]. The integrated diffraction patterns (I(Q)) exhibited two strong halos at around $Q = 26\,nm^{-1}$ and $Q = 44\,nm^{-1}$ (where Q is the absolute value of the wave-vector: $Q = 4\pi \sin\theta/\lambda$) and some additional undulations, similarly to that of the as-cast alloy. A clear shift of the halos in the diffraction patterns was observed between a selected reference position (see Fig. 1) and the measurement positions. In order to quantify this shift (Q_{shift}), the $\Phi(\hat{Q}) = \int \left| I_{ref}(Q) - I(Q + \hat{Q}) \right| dQ$ function was minimized for $\hat{Q}$ giving the accurate $Q_{shift} = \hat{Q}$ in the minimum. The detailed evaluation procedure can be found in recent publications [8,14].

As seen in Fig. 2, the relative shift (Q_{shift}/Q) of the first scattering halo increases monotonously with increasing strain rate up to $r = 1$ mm and $r = 2$ mm for $Zr_{57}Ti_5Cu_{20}Al_{10}Ni_8$ and $Zr_{44}Ti_{11}Cu_{10}Ni_{10}Be_{25}$, respectively, than it levels of followed by a drop at the perimeter of the disk. This kind of drop towards the edge of the disk is might be connected to the minor outflow of the material at the perimeter of the tools (see the optical image in Fig. 1) and was discussed elsewhere [14]. The shift of the halo positions during HPT deformation is associated with a stress induced average bond length change in the glassy structure. As was demonstrated recently, this bond length change strongly depends on the angle between the torsion axis and the X-ray beam, corresponding to a structural anisotropy in the material [8]. These structural changes can temporally persist beyond the glass transition in the viscous liquid as the results of the thermal analysis reflect in Fig. 3.

Fig. 3a shows a typical temperature program and the corresponding heatflow signal recorded during the TMDSC measurement. Fig. 3b presents the average heatflow signals corresponding to the as-cast $Zr_{44}Ti_{11}Cu_{10}Ni_{10}Be_{25}$ BMG and to the central and outer part of the HPT disk. As seen, each curve exhibits T_g followed by a supercooled region. The small exothermic prepeak (appears only at very low heating rates) corresponds to the formation of metastable quasicrystalline phase, while the main DSC peak is related to the simultaneous crystallization of several stable phases [15]. The deformation induced structural changes slightly decrease

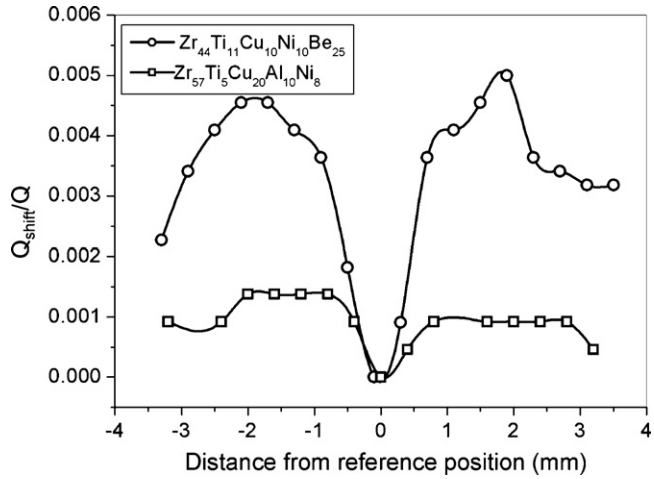

Fig. 2. Relative shift of the halo positions, Q_{shift}/Q for $Zr_{44}Ti_{11}Cu_{10}Ni_{10}Be_{25}$ and $Zr_{57}Ti_5Cu_{20}Al_{10}Ni_8$ measured along the diameter of the HPT disks.

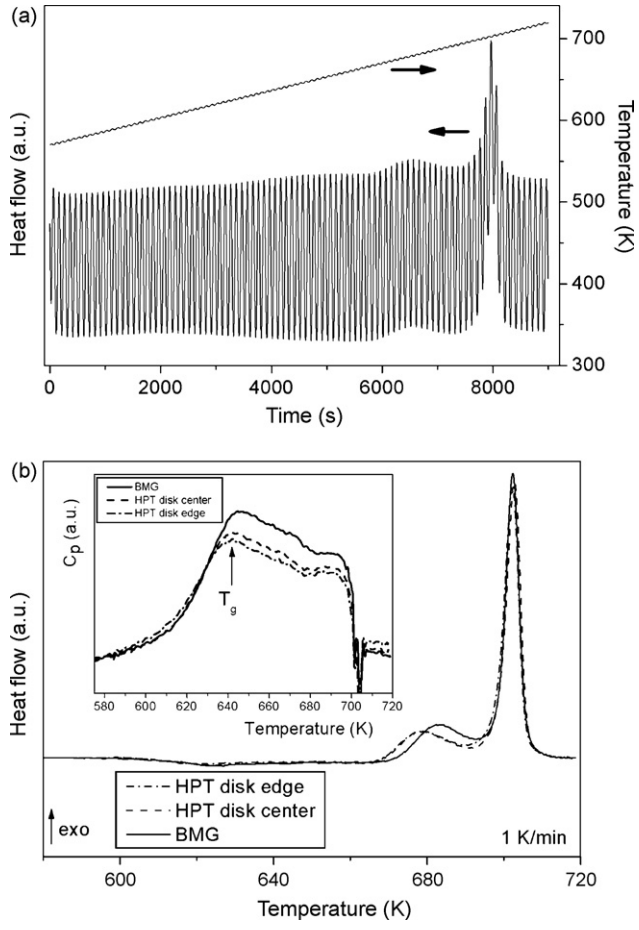

Fig. 3. (a) Temperature program and heat flow signal recorded during a TMDSC measurement. (b) Average heat flow signal (1 K/min heating rate) corresponding to the as-cast $Zr_{44}Ti_{11}Cu_{10}Ni_{10}Be_{25}$ BMG and to the central and outer part of the HPT disk. The inset shows the specific heat (C_p) as a function of temperature.

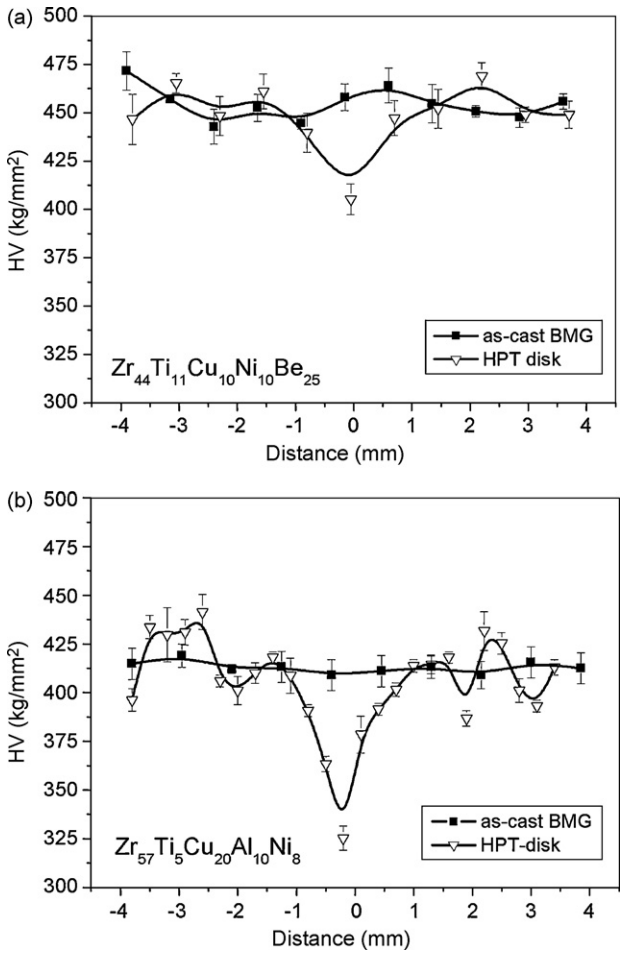

Fig. 4. Hardness (HV) values along the diameter of the as-cast BMG rod and HPT disks for (a) $Zr_{44}Ti_{11}Cu_{10}Ni_{10}Be_{25}$ and (b) $Zr_{57}Ti_5Cu_{20}Al_{10}Ni_8$.

the crystallization temperature of the first metastable phase and additionally exhibit a remarkable decrease of the C_p in supercooled liquid state, see the inset of Fig. 3b. This decrease in the C_p signal is an indicative of an order in the supercooled liquid state, which might originate from the structural anisotropy of the deformed glass.

Fig. 4a and b summarizes the HV data obtained from indentation measurements along the diameter of the as-cast BMG rods and HPT disks. As seen, the average hardness of the as-cast $Zr_{44}Ti_{11}Cu_{10}Ni_{10}Be_{25}$ (450 kg/mm^2) is somewhat larger than that of the $Zr_{57}Ti_5Cu_{20}Al_{10}Ni_8$ alloy (412 kg/mm^2). Commonly, at the perimeter of the HPT disks, the HV values fluctuate around the average hardness of the as-cast samples, while a 10–20% decrease can be observed in the in the center of the disks. This kind of deformation induced softening is a consequence of extreme shear localization [4]. Recent numerical simulations suggest that the temperature can increase significantly during torsional straining, especially out of the center of the disk [16], which can homogenize the plastic deformation. This homogeneous shear is responsible for the observed bond length change which is hardly detectable for the areas with extreme shear localization.

4. Conclusions

$Zr_{44}Ti_{11}Cu_{10}Ni_{10}Be_{25}$ and $Zr_{57}Ti_5Cu_{20}Al_{10}Ni_8$ bulk metallic glass disks have been subjected to severe plastic deformation by high pressure torsion. Focused synchrotron X-ray diffraction measurements along the diameter of the disks revealed no evidence of nanocrystallization, however, a monotonously increasing shift in the first amorphous halo position reflects structural changes in the glass. TMDSC scans confirmed a minor decrease in the stability of the deformed sample accompanied by a remarkable decrease of the C_p in supercooled liquid state. Due to the plastic deformation, a softening takes place only at the center of the disk, while the outer part has the same hardness value as that of the as-cast BMG.

Acknowledgements

We appreciate the support of the Hungarian Scientific Research Fund under grant No. 67893. Á.R. is indebted for the Bolyai Scholarship of the Hungarian Academy of Sciences. The authors thank the HPT disks for Dr. E. Schafler and the Erich Schmid Institute, Leoben, Austria. We also acknowledge the European Synchrotron Radiation Facility for provision of synchrotron radiation facilities and we would like to thank Dr. Jonathan Wright for assistance in using beamline ID 11.

References

[1] A. Inoue, Acta Mater. 48 (2000) 279.
[2] F. Spaepen, Acta Metall. 25 (1977) 407.
[3] A.S. Argon, Acta Metall. 27 (1979) 47.
[4] H. Bei, S. Xie, E.P. George, Phys. Rev. Lett. 96 (2006) 105503.
[5] A.R. Yavari, A. Le Moulec, A. Inoue, N. Nishiama, N. Lupu, E. Matsubara, W.J. Botta, G. Vaughan, M. Di Michiel, A. Kvick, Acta Mater. 53 (2005) 1611.
[6] Y. Zhang, W.H. Wang, A.L. Greer, Nat. Mater. 5 (2006) 857.
[7] X.K. Xi, D.Q. Zhao, M.X. Pan, W.H. Wang, Y. Wu, J.J. Lewandowski, Phys. Rev. Lett. 94 (2005) 125510.
[8] Á. Révész, E. Schafler, Zs. Kovács, Appl. Phys. Lett. 92 (2008) 011910.
[9] R.Z. Valiev, Y. Estrin, Z. Horita, T.G. Langdon, M.J. Zehetbauer, Y.T. Zhu, JOM-J. Miner. Met. Mater. Soc. 58 (2006) 33.
[10] A. Peker, W.L. Johnson, Appl. Phys. Lett. 63 (1993) 2342.
[11] A.P. Zhilyaev, T.G. Langdon, Prog. Mater. Sci. 53 (2008) 893.
[12] A. Hammersley, S.O. Svensson, A. Thompson, Nucl. Instrum. Methods A: Accelerators Spectrometers Detectors Assoc. Equip. 346 (1994) 312.
[13] W.C. Oliver, G.M. Pharr, J. Mater. Res. 7 (1992) 1564.
[14] Zs. Kovács, E. Schafler, Á. Révész, J. Mater. Res. 23 (2008) 3409.
[15] J. Gubicza, J.L. Lábár, E. Agócs, D. Fátay, J. Lendvai, Scripta Mater. 58 (2008) 291.
[16] S. Hóbor, Á. Révész, P.J. Szabó, A.P. Zhilyaev, V. Kovács Kis, J.L. Lábár, Zs. Kovács, J. Appl. Phys. 104 (2008) 033525.